Research Article

MODELING OF ASYNCHRONOUS UNITS OF A POWERFUL PUMPING STATION IN THE PRESSURE STABILIZATION MODE

Vladyslav LYSIAK[1,*]

[1]Department of Electric Power Engineering and Control Systems, Institute of Power Engineering and Control Systems, Lviv Polytechnic National University, 12 Bandera Street, Lviv, 79013, Ukraine

vladyslav.h.lysiak@lpnu.ua

*Corresponding author: Vladyslav Lysiak; vladyslav.h.lysiak@lpnu.ua

DOI: 10.15598/aeee.v23i2.240807

Article history: Received Aug 15, 2024; Revised Dec 19, 2024; Accepted Mar 15, 2025; Published Jun 30, 2025.

Abstract. *The paper is devoted to developing a mathematical model of a powerful controlled pumping station with automatic pressure stabilization. The work aims to increase the efficiency of the liquid transportation process through main and large distribution pipelines. The proposed model with a comparable level of detail describes the electromechanical and hydraulic subsystems as a single entity. The equations of the hydraulic subsystem are formed based on the principle of electrohydrodynamic analogy and reflect the physical processes in its components. The parameters of the centrifugal pump model were calculated based on the geometry and dimensions of its internal elements, taking into account the influence of the physical properties of the working fluid. It makes it possible to conduct a comprehensive study of such objects without physical impact on them, taking into account the mutual dependence of both subsystems and changes in the parameters of the elements of the hydraulic subsystem. The paper offers directions for use and ways to improve the functionality of the developed model.*

Keywords

Centrifugal, control, induction, model, motor, pipeline, pump, station, system.

1. Introduction

Powerful pumping stations (PS) of main and large distribution pipelines (PL) are strategically important. They ensure the movement of large volumes of liquid [1] and consist of inextricably linked electromechanical and hydraulic subsystems. Power overspends due to non-optimal modes of individual powerful units, suboptimal numbers of less powerful units operating simultaneously, and transient processes are quite significant. According to [2], they can reach 14% of the total energy consumption of the PS. According to the same data, up to 16 pumping units (PU) can occur switching at the main oil station in just one day. Overspends of electricity at the substation also lead to significant overspends in the elements of electrical networks. The high cost of electricity and equipment and the inadmissibility of work interruptions complicate and usually make it impossible to carry out physical experiments on operating powerful PS. Therefore, the development of non-contact means of computer prediction of operating modes, fault finding, and automatic control systems for operating such objects is actual.

Multi-unit electric-driven PS consists of inextricably linked electromechanical and hydraulic subsystems that influence each other. In turn, the hydraulic subsystem is characterized by the mutual influences of hydraulically connected individual CPs and a common PL. The electromechanical subsystem is also characterized by the mutual influences of the electric drives of these CPs electrically connected to a common power supply centre. Thus, the operating modes of other units of both the hydraulic and electromechanical subsystems depend on the operating mode of an individual unit. Therefore, for a comprehensive analysis of the operating modes of the PS, it must be considered an integral electrotechnological complex with a comparable detailing of the representation of its components.

One of the tasks of controlling PS modes is to maintain constant pressure in a given node of the hydraulic subsystem at different levels of fluid consumption. The most common methods of such control are switching units and changing the operating conditions of centrifugal pumps (CP). The latter can be carried out, in particular, by changing the characteristics of the hydraulic network (throttling or bypassing of CP), as well as by frequency control of the engines of the PU. Throttling or bypassing leads to a decrease in the energy efficiency of pumping. The maximum energy efficiency of the PS can be achieved by changing several simultaneously operating PUs and the frequency control of one of them. Such a control system and the algorithm of its operation are presented in [3]. However, its functionality is limited only to steady-state modes. In addition, only the volume flow rate of the working fluid is measured to stabilize the pressure, which is ineffective for stabilizing the pressure in dynamic modes. The specified limitations are absent in the model [4]. However, an approximate polynomial represents the hydraulic subsystem. This makes it impossible to study the processes in the hydraulic subsystem. Most of the other works devoted to PS (for example [5–7], and [8]) are also characterized by extremely simplified representations of one or both subsystems. In many works, the braking fan mechanical torque describes the hydraulic subsystem with CP. In [9] it is shown that this approach is correct only under the condition of constant parameters of the hydraulic subsystem. In the general case, the parameters of CP depend on the physical properties of the working fluid, the spatial structure of the elements of the hydraulic subsystem, and the pumping mode.

Among the large number of works devoted to CP, in our opinion, it is advisable to single out those in which the mathematical model of CP is based on its spatial structure, which cannot reflected by scalar models. In particular, the authors of [10] showed that the projections of the force acting on the liquid at the outlet of the rotating impeller onto fixed axes are harmonic time functions. To describe the motion of the fluid in the flow part of the CP impeller, the modified Euler equation was used, and in the spiral part, the Navier-Stokes differential equations. The latter allowed the authors to write the equations of the complex CP model in orthogonal *d-q* coordinates rigidly connected to the impeller. This made it possible to operate with CP regime parameters that are constant in time and to determine the dissipative and inertial hydraulic resistances of CP through the design parameters and physical characteristics of the working fluid. It should be noted that the ratio of dissipative and inertial hydraulic resistances CP is one of the forms of the Reynolds number, which determines the fluid motion regime. Considering the physical content, adaptability to the application of the theory of circles, and the form of writing the model equations common in traditional electric power engineering [10], we took it as a basis. The improved model was successfully applied in the publication devoted to steady-state regimes [3] and during the modelling of dynamic regimes [11]. These allow the consideration of the impact of operational and emergency changes in CP internal parameters on the PS's operating modes. The model [11] makes it possible to study the mutual influence of electromechanical and hydraulic processes and parameters. However, it does not have any unit control system. The analysis of the above and other works gives grounds to conclude that there is no mathematical model of a powerful PS with a closed frequency pressure control system and a comparable level of detail of the mathematical description of the electromechanical and hydraulic subsystems. The paper is devoted to developing a mathematical model of a powerful regulated pumping station with automatic pressure stabilization.

2. Mathematical Model

Figure 1 shows the structural diagram of the PS with a closed frequency pressure control system. Two aggregates are hydraulically connected in series: support (PU_1) and main (PU_2).

The main unit provides the necessary pressure in the given range of flow of the working fluid. Its power is 5-10 times greater than that of a support, and it has a much higher cost. CP blades are very sensitive to hydrodynamic cavitation, which destroys them. Both experimental [12] and theoretical [13] studies are devoted to the early detection of cavitation on CP blades. To avoid cavitation, a support unit is used. It creates a small constant pressure at the entrance of the main CP and provides a volumetric flow rate no less than the main unit provides. To stabilize the pressure PS within the required value H_{ref}, the current value of the pressure at the entrance to the PL is used. The sensor (SP) measures this pressure. From the output of the PI controller with parameters , and the signal is sent to the control system (CS). It provides frequency and voltage converter (FVC) formation of the frequency and voltage of the power supply voltage of the IM main PU. The main unit's supply voltage is formed based on the law of proportional frequency controlling IM. $v_{s_2}/f_{s_2} = const$ The IM of the support PUs is uncontrollable. For simplicity, we assume that both PUs are powered by three-phase symmetrical voltage sources that do not contain higher harmonics. The voltage and frequency of the supply voltage IM of the support PU are constant.

The model equations are written in a per-unit system. The following system of basis values was used to write the IM equations:

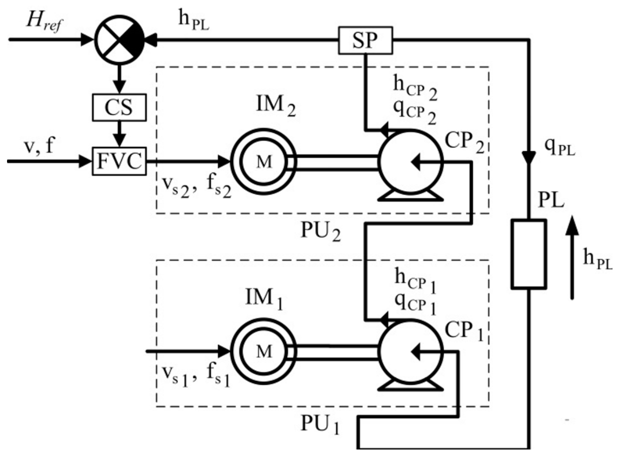

Fig. 1: The structural diagram of the PS.

$\omega_{IM.b} = \omega_{syn}$; $V_{IM.b} = \sqrt{2/3}V_{IM.nom}$; $I_{IM.b} = \sqrt{2}P_{IM.nom}/\left(\sqrt{3}V_{IM.nom}\eta_{IM.nom}cos\phi_{IM.nom}\right)$; $S_{IM.b} = (3/2)\,V_{IM.b}/I_{IM.b}$; $T_{IM.b} = S_{IM.b}/\omega_{IM.b}$; $Z_{IM.b} = V_{IM.b}/I_{IM.b}$, where ω_{syn}, $V_{IM.nom}$, $P_{IM.nom}$, $\eta_{IM.nom}$, $cos\phi_{IM.nom}$ are nominal passport parameters of IM. The IM equations are formed based on the generalized equations of the electromechanical converter, taking into account the following assumptions: the temperature regime is stable, the winding parameters are concentrated; the weber-ampere characteristic of the magnetic system is non-linear; the influence of the shape of the core on the distribution of the magnetic field is not taken into account. The following system of basis values was used to write the CP equations: $\omega_{CP.b} = \omega_{CP.nom}$; $H_{CP.b} = H_{CP.nom}$; $Q_{CP.b} = Q_{CP.nom}$; $S_{CP.b} = \rho g H_{CP.b} Q_{CPp.b}$; $T_{CP.b} = S_{CP.b}/\omega_{CP.b}$; $Z_{CP.b} = \rho g H_{CP.b}/Q_{CPp.b}$, where $\omega_{CP.nom}$, $H_{CP.nom}$, $Q_{CP.nom}$ are the nominal passport parameters of CP, ρ, g are the density of the working fluid and free-fall acceleration. The CP equations are formed based on an electrohydrodynamic analogy according to the complex substitution scheme [10], taking into account the following assumptions: the temperature regime is stable, the working fluid is homogeneous with a constant density, the image vectors of the volumetric flow rate and pressure of the working fluid at the outlet of the impeller are collinear.

We consider the IM rotor, the CP impeller, and the common shaft to be rigid. For the basic value of the frequency common to both subsystems, we take the basic value of the IM frequency: $\omega_b = \omega_{IM.b}$. PU equations are formed in orthogonal d-q coordinates rigidly connected to the common shaft. Complex variables included in the equations are marked with a dot above. Coordinate d corresponds to the real component, and coordinate q corresponds to the imaginary component. The differential equations have been solved to the first derivatives, which may be convenient for use in computer mathematics systems.

$$\dot{h}_0 = H_{0.nom}\left(\frac{\omega_b}{\omega_{CP.b}}\right)^2 \omega_r^2 e^{j\omega_b \omega t}, \tag{3}$$

$$h_{CPd}q_{33q} - h_{CPq}q_{33d} = 0, \tag{4}$$

$$\begin{aligned}\frac{\mathrm{d}\omega_r}{\mathrm{d}t} &= \frac{1}{J_\Sigma \omega_{IM.b}} \cdot \left(T_{IM.b}\left(\psi_{\delta d} i_{sq} -\right.\right.\\ &- \psi_{\delta q} i_{sd}) - T_{CP.b} H_{0.nom} \frac{\omega_{IM.b}}{\omega_{CP.b}} \omega_r \times \\ &\times \left.\sqrt{\left(q_{11d}+q_{44d}\right)^2 + \left(q_{11q}+q_{44q}\right)^2}\right),\end{aligned} \tag{5}$$

$$q_{33d_1}^2 + q_{33q_1}^2 = \left(\frac{Q_{CPb_2}}{Q_{CPb_1}}\right)^2 \left(q_{33d_2}^2 + q_{33q_2}^2\right), \tag{6}$$

$$q_{PL} = \sqrt{q_{33d_1}^2 + q_{33q_1}^2}, \tag{7}$$

$$h_{PL} = \sqrt{h_{CPd_1}^2 + h_{CPq_1}^2} + \frac{H_{CPb_2}}{H_{CPb_1}}\sqrt{h_{CPd_2}^2 + h_{CPq_2}^2}, \tag{8}$$

$$\frac{\mathrm{d}q_{PL}}{\mathrm{d}t} = -\frac{r_{PL}}{L_{PL}} q_{PL} + \frac{1}{L_{PL}} h_{PL} - \frac{1}{L_{PL}} h_{st}, \tag{9}$$

$$\frac{d\omega_{s_2}}{dt} = \frac{1}{2\omega_{s_2}}\left(I\left(H_{ref} - h_{PL}\right) - Py\right), \tag{10}$$

$$\frac{dh_{PL}}{dt} = y, \tag{11}$$

$$v_{sd_2} = \omega_{s_2}, \tag{12}$$

where t is time in (s); ω_s, ω_r are synchronous sycircular frequency of the stator winding voltage IM and the circular speed of rotation of the common shaft; $\dot{v}_s$, $\dot{i}_s$, and $\dot{i}_r$ are stator voltage and current, as well as rotor current IM reduced to the stator winding; ψ_δ is reduced to the winding of the stator flux coupling from the magnetic flux of the air gap IM; R_s, $L_{\sigma s}$, R_r, $L_{\sigma r}$, R_a are IM parameters; $\dot{h}_0$ is fictitious pressure of the idealized CP; $\dot{q}_{11}$, $\dot{q}_{22}$, $\dot{q}_{33}$, $\dot{q}_{44}$ are fictitious costs of CP; h_{PL}, q_{PL} are pressure and volume flow rate of liquid at PL inlet; h_{st} is static counter pressure PL; $r_{mech}\left(q_{PL}\right)$ is equivalent nonlinear hydraulic resistance, which takes into account dissipative losses of mechanical energy in CP depending on its pumping mode [14]; r_{11}, r_{12}, r_{13}, r_{21}, r_{22}, r_{23}, r_{31}, r_{32}, r_{33}, L'_{11}, L'_{12}, L'_{13}, L'_{21}, L'_{22}, L'_{23}, L'_{31}, L'_{32}, L'_{33} are dissipative hydraulic resistances and inertial hydraulic inductances CP, which are calculated by the size of its internal elements and physical characteristics of the working fluid according to the method [10], and [11]; r_{PL}, L_{PL} are dissipative hydraulic resistance and inertial hydraulic inductance PL; J_Σ is inertia PU in (kgm^2). The magnetic reluctance of the IM is presented in the form of an approximation polynomial $R_m\left(\psi_\delta\right) = I_{mn}\left(a_0 + a_2\left(\psi_{\delta d}^2 + \psi_{\delta q}^2\right) + a_4\left(\psi_{\delta d}^2 + \psi_{\delta q}^2\right)^4\right)$, where a_0= 0.82; a_2= 0.148; a_4= 0.044; $I_{mn} = 1/(x_\sigma + x_a)$, where x_σ, x_a are relative inductances of dispersion and magnetization of the IM in the nominal mode. In this case, we neglect the effect of frequency on a R_m, since

$$\left|\begin{array}{c}\frac{d\dot{i}_s}{dt}\\ \frac{d\dot{i}_r}{dt}\\ \frac{d\dot{\psi}_\delta}{dt}\\ 0\end{array}\right| = \left\|\begin{array}{cccc}-\frac{R_s}{L_{\sigma s}}-j\omega_s & 0 & -\frac{1}{L_{\sigma s}} & -j\frac{\omega_s}{L_{\sigma s}}\\ 0 & -\frac{R_r}{L_{\sigma r}}-j(\omega_s-\omega_r) & \frac{\omega_s}{L_{\sigma r}} & j\frac{\omega_s-\omega_r}{L_{\sigma r}}\\ 0 & 0 & 1 & 1\\ 0 & 1 & 1 & -R_m(\psi_\delta)-j\frac{\omega_s}{R_a}\end{array}\right\| \times \left|\begin{array}{c}\dot{i}_s\\ i_r\\ \dot{e}_s\\ \dot{\psi}_\delta\end{array}\right| + \left|\begin{array}{c}\dot{v}_s\\ 0\\ 0\\ 0\end{array}\right|, \tag{1}$$

$$\left|\begin{array}{c}\frac{d\dot{q}_{11}}{dt}\\ \frac{d\dot{q}_{22}}{dt}\\ \frac{d\dot{q}_{33}}{dt}\\ \frac{d\dot{q}_{44}}{dt}\end{array}\right| = \left\|\begin{array}{cccc}\frac{r_{11}}{L'_{11}}-\frac{r_{21}}{L'_{12}} & \frac{r_{22}}{L'_{12}}-\frac{r_{32}}{L'_{13}} & \frac{r_{33}}{L'_{13}}-\frac{r_{23}}{L'_{12}} & 0\\ \frac{r_{11}}{L'_{21}}-\frac{r_{21}}{L'_{22}} & \frac{r_{22}}{L'_{22}}-\frac{r_{32}}{L'_{23}} & \frac{r_{33}}{L'_{23}}-\frac{r_{23}}{L'_{22}} & 0\\ \frac{r_{11}}{L'_{31}}-\frac{r_{21}}{L'_{32}} & \frac{r_{22}}{L'_{32}}-\frac{r_{32}}{L'_{33}} & \frac{r_{33}}{L'_{33}}-\frac{r_{23}}{L'_{32}} & 0\\ 0 & 0 & 0 & -\frac{r_{mech}(q_{PL})}{L_{mech}}\end{array}\right\| \times \left|\begin{array}{c}\dot{q}_{11}\\ \dot{q}_{22}\\ \dot{q}_{33}\\ \dot{q}_{44}\end{array}\right| + \left|\begin{array}{c}\frac{1}{L_{11}}\\ \frac{1}{L_{21}}\\ \frac{1}{L_{31}}\\ \frac{1}{L_{mech}}\end{array}\right| \times \dot{h}_0, \tag{2}$$

it becomes significant at frequencies above 100 Hz [15]. The device's maximal operating frequency is the synchronous frequency of the electrical power supply system (in this case 50 Hz).

Equation (1) describes the electromechanical subsystem. Equations (2), (3), and (4) describe the hydraulic PU subsystem. In particular, equation (4) specifies the collinearity of the image vectors of the real head and the real flow at the outlet of the CP. Equation (5) of the PU common shaft motion combines the electromechanical and hydraulic coordinates of the IM and CP modes. Equations (1), (2), (3), (4) and (5) are written separately for each PU. Equations (6), (7), (8), and (9) describe the hydraulic connections of PU and PL. Equations (10), (11), and (12) determine the stabilization of the PS head. The basis is taken to ensure a constant ratio of the nominal voltage to the nominal frequency of the voltage of the stator winding of the electric motor. Taking this into account, in this particular case, in the per-unit system, the law of proportionality of the control frequency of the main unit's induction motor is determined by the expression $v_{s_2}/f_{s_2} = 1$. In the mathematical model, this is presented as equation (12). In general, equations (10), (11), and (12) can be replaced by other appropriate equations that describe another specific control system. It should be noted that the dissipative hydraulic resistance of the CP depends not only on its internal dimensions but also on the kinematic viscosity of the liquid. In turn, the kinematic viscosity of the liquid depends on the temperature. Thus, it is possible to take into account the influence of temperature conditions on the PS's operating modes.

3. Test Calculations

To verify the model, test simulations of the operating modes of the units were carried out for 200 seconds. The nominal power of the motor is selected based on the nominal power of the pump. The pump passport indicates the nominal useful hydraulic power of the pump at the outlet of the impeller. The required me-

Tab. 1: Parameters of IM 4AN355M6U3 of the supporting PU.

P_{nom}, kW	η_{nom}	$V_{s.nom}$, V	n_{nom}, rpm	$\cos\varphi_{nom}$
250	0.935	380	985	0.9
p_0	T_{max^*}	T_{min^*}	T_{s^*}	I_{s^*}
3	2.2	0.9	1.4	7

Tab. 2: Parameters of IM 4AZMV-1600/6000U2 of the main PU.

P_{nom}, kW	η_{nom}	$V_{s.nom}$, V	n_{nom}, rpm	$\cos\varphi_{nom}$
1600	0.961	6300	2979	0.9
p_0	T_{max^*}	T_{min^*}	T_{s^*}	I_{s^*}
1	2.6	0.7	1.9	6

Tab. 3: Parameters of CP 14NDs-N of the supporting PU.

H_{nom}, m	Q_{nom}, $m^3 \cdot h^{-1}$	η_{nom}	n_{nom}, rpm	$P_{hydr.nom}$, kW
45	1260	0.809	980	154
$H_{0.nom^*}$	$R_{\Delta Q^*}$	$L_{\Delta Q^*}$	$R_{\Delta H^*}$	$L_{\Delta H^*}$
1.302	29.47	9.49	$6.627 \cdot 10^{-4}$	0.4144
L_{t^*}	$L_{\mu H^*}$	$L_{\mu Q^*}$	R_{m^*}	L_{mech^*}
0.00876	0.0352	0.2375	7.180	0.02287

Tab. 4: Parameters of CP QG300-2-100b of the main PU.

H_{nom}, m	Q_{nom}, $m^3 \cdot h^{-1}$	η_{nom}	n_{nom}, rpm	$P_{hydr.nom}$, kW
428	800	0.745	2980	932
$H_{0.nom^*}$	$R_{\Delta Q^*}$	$L_{\Delta Q^*}$	$R_{\Delta H^*}$	$L_{\Delta H^*}$
2.641	43.89	15.12	$5.897 \cdot 10^{-5}$	0.4675
L_{t^*}	$L_{\mu H^*}$	$L_{\mu Q^*}$	R_{m^*}	L_{mech^*}
1.03311	0.3122	2.3111	20.377	0.00436

chanical power of the drives of the pumps given in the manuscript is significantly higher since the efficiency of the specified pumps is quite low (0.809 for the support pump and 0.745 for the main one). The nominal power of the electric motors used in this case is overestimated. To verify the modelling, we used the nominal parameters of the installed equipment of one of the operating powerful oil pumping stations. For verifying the operability and adequacy of the model, the simplest scalar automatic pressure stabilization system based on a proportional frequency control law was chosen. The time diagrams shown in Fig. 2 display the main results of the test simulation. In particular, the electromechanical parameters of the mode are shown in Fig. 2(a), 2(b), 2(c), and 2(d), and the hydraulic parameters are shown in Fig. 2(e), and 2(f). Figure 2(d) shows the electromagnetic moments IM. Figure 2(e) shows the pressures of individual CPs (on different scales). Figure 2(f) shows the pressure and volumetric flow rate of the PS working fluid (the CP flow rate and the PS flow rate are equal). The graphs also show the catalogue nominal parameters of IM and CP.

The set value of the PS pressure, which was subject to stabilization, was 473 m. It was equal to the sum of the nominal pressures of the supporting CP (45 m) and the main CP (428 m). During the simulation, the flow rate of the working fluid was changed five times. By the time of 3 s, the pipeline was completely blocked. After that, the fluid flow rate was set at 105 dm^3/s (47% of the nominal flow rate of the main unit). At the time points of 40 s and 70 s, the consumption increased by 43% of the previous value each time – to 150 dm^3/s and to 215 dm^3/s, respectively, and at the time points of 100 s and 130 s – it decreased to 150 dm^3/s and 105 dm^3/s respectively. At the moment 179 s there was an interruption of the power supply of both units and their subsequent stop. To check the operability of the model, all changes in pipeline parameters took place within 0.1 s, corresponding to the speed of development of emergency modes. This led to corresponding fluctuations in pressure and liquid flow. At the same time, the PS pressure was successfully maintained at the level of the set value. It should be noted that under normal operating conditions, the pipeline parameters change smoothly and slowly, which does not lead to such intense fluctuations. There is only simulation verification in the work. The lack of open access to both experimental data and power equipment of powerful pumping stations due to their strategic importance and the inadmissibility of interrupting their work explain this. For the model's testing, we gave fast perturbations of the volumetric flow rate with large amplitude. The results of the mathematical experiment, shown in Fig. 2, showed the stability of the control and the reliability of the model. Each disturbance caused hydraulic and electromechanical transients, which quickly and steadily ended in normal exploitation steady-state regimes. The adequacy of the modelling is evidenced by the analysis of the transient modes of equipment, as well as the coincidence of the indicators of the steady-state modes, which complete the transient modes, and the corresponding catalogue parameters of the equipment. The development and comparison of the efficiency of specific configurations of the pressure stabilization systems were not the purpose of this work and are planned in further research.

4. Conclusion

A mathematical model of asynchronous PUs of a powerful PS in the pressure stabilization mode was developed and verified. The equations of the hydraulic subsystem are formed based on the principle of electrohydrodynamic analogy and reflect the physical processes in its internal elements. This made it possible to use the theory of electric circuits to write the equations of not only electromechanical but also hydraulic subsystems. The composition of models of electromechanical and hydraulic subsystems into a single whole with comparable detailing of their elements allows simultaneous research of processes in these subsystems, directly calculating and analysing the energy, electromagnetic and hydraulic coordinates of the mode, investigating their mutual influence, evaluating both the state of individual elements of the units and the state of the units as a whole. The calculation of the parameters of the CP model is based on the geometric dimensions of the internal elements of the CP, as well as the physical properties of the working fluid. Therefore, during simulation, it is possible to investigate the impact of operational and emergency deviations of these factors both on the regimes of fluid transportation systems and on the regimes of their electrotechnical complexes. Increasing the efficiency of existing powerful PS is possible by optimizing the operating modes. The developed model makes it possible to conduct studies of regimes without a physical experiment on expensive operating equipment. Thanks to this, there will be no disruption of its operation and interruptions in the transportation of liquid, eliminating the risks of accidents and financial losses. The model can be integrated into automated design systems of powerful pumping stations and used during the search for optimal design solutions. The potential ability to reproduce in the developed mathematical model various typical methods of controlling the flow and head of CP units will allow for an effective technical and economic comparison of control options both at the design stage of new and during the modernization of existing pumping stations. A promising direction of improvement of the developed mathematical model may be to transform it into a hydride model by supplementing it with a physical system of automatic control, which will significantly increase

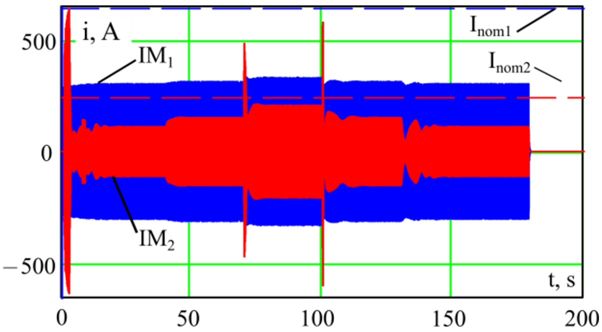

(a) Stator current of IM.

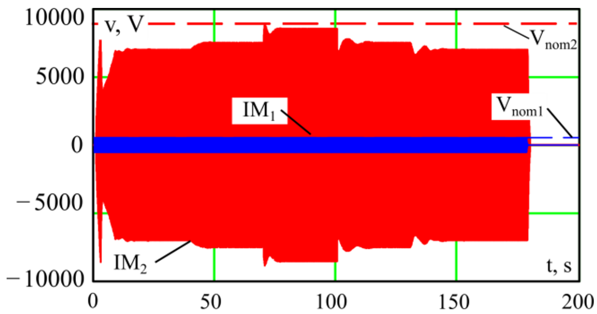

(b) Stator voltage of IM.

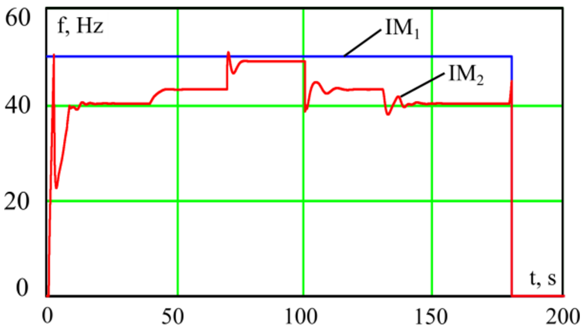

(c) Frequency of stator voltage of the IM.

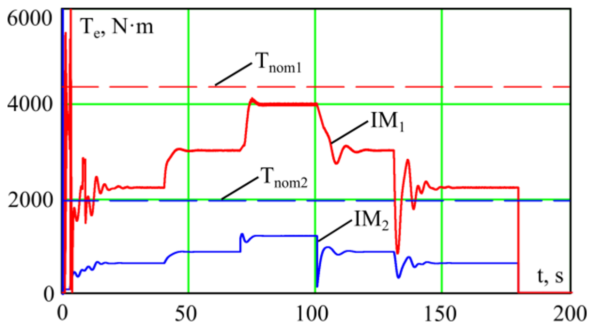

(d) Electromagnetic torque of IM.

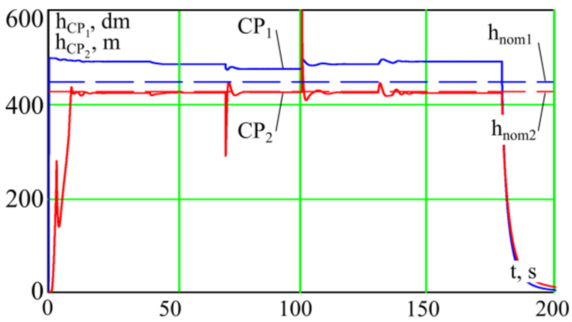

(e) Pressure of CP.

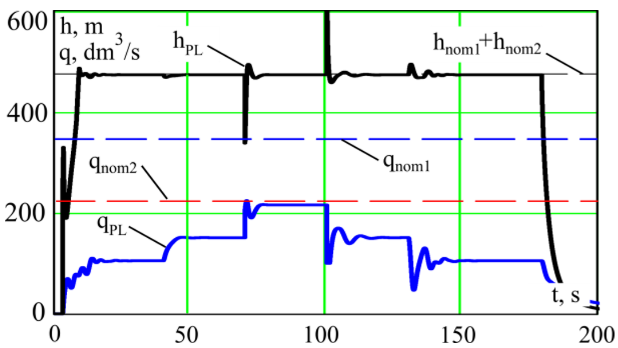

(f) Volumetric flow rate and pressure of the PS.

Fig. 2: Main results of the test simulation

its functionality. The composition of the created model with a model of a hydraulic heat network can also become an effective tool for a comprehensive study of the mutual influence of thermal, hydraulic, and electromechanical processes that occur in centralized heat supply systems.

References

[1] PULIDO-CALVO, I., J. C. GUTIERREZ-ESTRADA. Selection and Operation of Pumping Stations of Water Distribution Systems. *Environmental Research Journal*. 2011, vol. 5, iss. 3, pp. 1-20. http://www.uhu.es/juanc.gutierrez/articuloPDF/ERJ2011.pdf.

[2] BOHDANOV, R. Methodic of electric energy consumption pattern calculation in oil transportation via pipelines. *Electronic scientific journal "Oil and Gas Business"*. 2012, iss. 1, pp. 58-68. https://elibrary.ru/item.asp?id=20709396. http://ogbus.ru/files/ogbus/authors/Bogdanov/Bogdanov_3.pdf.

[3] PARANCHUK, Y., V. LYSIAK. Energy efficient power supply system and automatic control of modes of the “power supply – pumping station”

complex. *Naukovyi Visnyk Natsionalnoho Hirnychoho Universytetu*. 2015, iss. 3, pp. 115-124. DOI: 10.29202/nvngu/2018-3/16.

[4] KUTSYK, A., A. LOZYNSKYI, O. KINCHUR. Mathematical model of the system "frequency-controlled electric drive - pump - water supply network". *Bulletin of the Lviv Polytechnic National University. Series of Electrical Power and Electromechanical Systems*. 2015, iss. 834, pp. 48–55. http://nbuv.gov.ua/UJRN/VNULPEEC_2015_834_10.

[5] GOMROKCHI, U., R. PARVARESH. Flexibility of energy and water management in pressurized irrigation systems using dynamic modeling of pump operation. *Environment, Development and Sustainability*. 2021, vol. 23, pp. 18232–18251. DOI: 10.1007/s10668-021-01436-7.

[6] JANEVSKA, G. Mathematical Modeling of Pump System. *In: Electronic International Interdisciplinary Conference*. 2013, vol. 2, pp. 455–458. https://www.researchgate.net/publication/283348821_Mathematical_Modeling_of_Pump_System.

[7] WANG. Y., H. ZHANG, Z. HAN, X. NI. Optimization Design of Centrifugal Pump Flow Control System Based on Adaptive Control. *Processes*. 2021, vol. 9, no. 9. DOI: 10.3390/pr9091538.

[8] SALMASI, F., J. ABRAHAM, A. SALMASI. Design Considerations for Pumping Stations Using Variable Speed Pumps. *Novel Perspectives of Engineering Research*. 2022, vol. 10, pp. 98–118. DOI: 10.9734/bpi/nper/v10/2220B.

[9] LYSIAK, V., M. OLIINYK, Y. SHELEKH. Modeling of Hydraulic Load of Electric Drive in Electrical Complex of Pumping Station. *Energy Engineering Control Systems*. 2018, Vol. 4, No. 1, pp. 31–36. DOI: 10.23939/jeecs2018.01.031.

[10] KOSTYSHYN, V., I. YAREMAK, P. KURLYAK. Creation of object-oriented model of centrifugal pump on the basis of electrohydrodynamic analogy method. *Naukovyi Visnyk Natsionalnoho Hirnychoho Universytetu*. 2019, iss. 6, pp. 72-79. DOI: 10.29202/nvngu/2019¬6/11.

[11] LYSIAK, V. Mathematical modeling of multi-units pumping station with asynchronous electric drive of centrifugal pumps. *Advances in Electrical and Electronic Engineering*. 2023, Vol. 21, no. 3, pp. 226–234. DOI: 10.15598/aeee.v21i3.4718.

[12] MOUSMOULIS, G., et al. Experimental analysis of cavitation in a centrifugal pump using acoustic emission, vibration measurements and flow visualization. *European Journal of Mechanics - B/Fluids*. 2019, vol. 75, pp. 300–311. DOI: 10.1016/j.euromechflu.2018.10.015.

[13] SUNAL, C. E., et al. Centrifugal Pump Fault Detection with Convolutional Neural Network Transfer Learning. *Sensors*. 2024, vol. 24, no. 8. DOI: 10.3390/s24082442.

[14] KOSTYSHYN, V., P. KURLYAK. Simulation of performance characteristics of centrifugal pumps by the electro-hydrodynamic analogy method. *Journal of Hydrocarbon Power Engineering*. 2015, vol. 2, iss. 1, pp. 24-31. https://www.ogpe.nung.edu.ua/index.php/jhpe/article/view/32.

[15] PUSTOVETOV, M., K. SOLTUS, I. SINYAVSKY. Computer modeling of induction motors and transformers. Examples of interaction with power electronic converters. *Saarbrücken (Germany): LAP LAMBERT Academic Publishing*. 2013. https://d-nb.info/1035545403.